Terahertz Vibration−Rotation−Tunneling Spectroscopy of the Ammonia Dimer. II. *A*−*E* States of an Out-of-Plane Vibration and an In-Plane Vibration

Wei Lin, Jia-xiang Han, Lynelle K. Takahashi, Jennifer G. Loeser,† and Richard J. Saykally*

Department of Chemistry, University of California, Berkeley, California 94720-1460

Received: April 2, 2007; In Final Form: May 30, 2007

Terahertz vibration−rotation−tunneling transitions have been measured between ca. 78.5 and 91.9 cm^{-1}, and assigned to *A*−*E* (ortho−para) combinations of NH_3 monomer states. The spectrum is complicated by inversion splittings that correlate to *E* symmetry monomer rovibronic states. Twenty progressions have been assigned to six excited states involving an out-of-plane vibration and an in-plane intermolecular vibration. The quality of the fit was affected by strong Coriolis interactions among these states and possibly an additional $K = 2$ state that was not explicitly observed in the data.

Introduction

Ammonia is one of the three textbook examples of hydrogen bonding. It had been generally assumed that all three corresponding gas-phase dimers $(HF)_2$, $(H_2O)_2$, and $(NH_3)_2$ have similarly bonded structure and rigidity, and indeed, both $(HF)_2$ and $(H_2O)_2$ have been found experimentally to be relatively rigid (when compared to van der Waals complexes), with near-linear hydrogen-bonded structures in the gas phase. It was not until the mid-1980s that the first high-resolution microwave spectra[1−3] revealed that $(NH_3)_2$ was dissimilar to $(HF)_2$ and $(H_2O)_2$. Since then, the ammonia dimer has attracted much attention from both experiment and theory. Notably, Loeser et al.[4] reported the complete far IR spectrum of the ground vibration−rotation−tunneling (VRT) states, in which they characterized the complex nature of the tunneling dynamics of the ammonia dimer, showing it to be one of the most nonrigid hydrogen-bonded complexes yet studied. We reviewed the recent experimental works in a recent paper.[5]

The extensive VRT spectroscopic works on the water dimer have helped the determination of its potential surface.[6−9] Leforestier et al.[10] developed a full dimensionality (12D) potential surface for the water dimer via direct inversion of spectroscopic data and used it to evaluate the equilibrium constant.[11] Most recently, Bukowski et al.[12] developed a force field of water entirely from first principles, which predicted excellent agreement with VRT experiments. It is now evidenced from both experimental and theoretical studies that the potential surface of the ammonia dimer is indeed extremely flat. Boese et al.[13] investigated the ammonia dimer using a novel density functional, which calculated the energy difference between the global minimum eclipsed C_s structure and the transition state C_{2h} structure to be only about 3.5 cm^{-1}. In order to proceed toward the ultimate goal of determining an accurate intermolecular potential surface like what has been done for the water dimer, it is necessary to thoroughly characterize the intermolecular vibrations. We recently reported the measurement and assignment of the VRT spectrum of $(NH_3)_2$ states correlating asymptotically to *A*−*A* symmetry monomer rovibronic states of an out-of-plane vibration.[5] In the present work, we extend the analysis to $(NH_3)_2$ states correlating asymptotically to *A*−*E* symmetry monomer states. Measurements were made for both $K = 0$ and 1 states. The spectra are complicated by strong Coriolis interactions between $K = 0$ and 1 states and inversion tunneling of the ammonia subunit correlating to *E* symmetry monomer rovibronic states. More than 900 transitions were measured and assigned for the ammonia dimer to both an out-of-plane vibration and an in-plane vibration. Transitions belonging to $(NH_3)_2$ *E*−*E* (para−para) states were also measured and assigned. A preliminary account was given by Loeser et al.[14] Figure 1 shows the recorded stick spectrum of the measured transitions.

The molecular symmetry group required to completely describe the VRT states of the ammonia dimer must contain all of the feasible permutation−inversion (PI) operations, which can be expressed as $3 \times 3 \times 2 \times 2 \times 2 \times 2 = 144$, where 3×3 refers to the three internal rotation positions of both ammonia subunits, 2×2 refers to the interchange of the two ammonia groups and the reflection in the assumed plane of symmetry, and the last 2×2 refers to the inversion tunneling of both ammonia groups. This corresponds to the molecular symmetry group G_{144}. In their analysis of the microwave spectrum of the ammonia dimer, Nelson and Klemperer[2] elegantly explored the nature of the tunneling states of $(NH_3)_2$ using group theoretical correlation diagrams. Assuming the C_s point group (the ammonia dimer with a plane of symmetry) for the rigid non-tunneling ammonia dimer, they identified G_{36} as the molecular symmetry group. This engendered a key question in interpreting the spectrum: Is the interchange tunneling much faster than the C_3 internal rotation (the $I + 2C_3$ limit), or does the opposite (the $2C_3 + I$ limit) hold? They concluded that $2C_3 + I$ was the correct limit. Coudert and Hougen[15] derived the energy level expressions for the general $(XY_3)_2$ systems of G_{36} symmetry, again assuming no inversion and "moderately high" barriers for all the internal motions. The complete characterization of the ground VRT state of the dimer by Loeser et al.[4] and the fully coupled six dimensional dynamical calculations of Olthof et al.[16,17] conclusively identified the complex tunneling dynamics of this extremely floppy cluster. These include (a) interchange tunneling, which exchanges the donor−acceptor roles of the two ammonia subunits, (b) internal rotation

* Corresponding author. Email: Saykally@berkeley.edu.
† Current address: Department of Chemistry, College of Marin, Kentfield, CA 94904.

10.1021/jp0725836 CCC: $37.00
Published on Web 09/07/2007

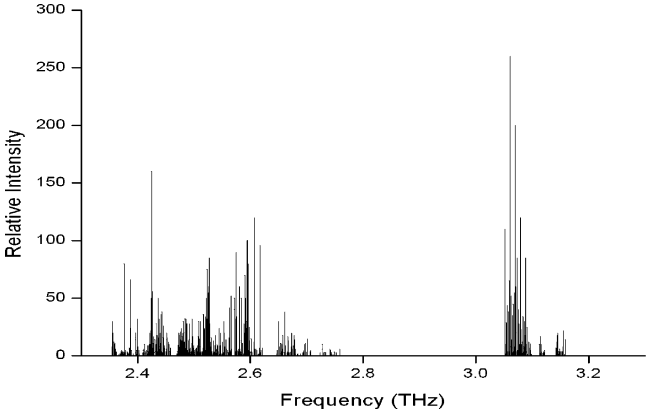

Figure 1. Stick spectrum of the currently scanned THz region. It should be noted that this is a composite spectrum, including transitions from several laser lines. Only the intensities of the transitions from the same laser line are comparable.

tunneling, which involves the rotation of each of the ammonia molecules along its C_3 symmetry axes, and (c) umbrella inversion tunneling of the ammonia monomers that correlate to E symmetry monomer rovibronic states. The determined inversion-tunneling splittings showed that the inversion tunneling of the ammonia in $(NH_3)_2$ is, although largely hindered, still observable in the spectra. Hence it is necessary to increase the number of PI operations of the G_{36} group by a factor of 2 $\times$ 2, making it the G_{144} group. These analyses ruled out the $2C_3 + I$ limit, and identified the $I + 2C_3 + i$ limit as the appropriate description of the tunneling dynamics. There have been some additional helpful discussions on this topic. Müller-Dethlefs and Hobza[18] used the ammonia dimer as an illustrative example in their review article on noncovalent interactions. Havenith[19] recently reviewed the experimental studies of the ammonia dimer. Bunker and Jensen[20] discussed the ammonia dimer in their book on molecular symmetry and spectroscopy.

Experimental Section

Terahertz VRT spectra of the ammonia dimer were observed in a continuous supersonic planar jet expansion probed by a tunable far-infrared (terahertz) laser spectrometer. The spectrometer has been described in detail elsewhere,[21,22] so only a brief description is given here. The tunable terahertz radiation is generated by mixing light from an optically pumped line-tunable far-infrared gas laser with continuously tunable frequency-modulated microwaves in a Schottky barrier diode to generate light at the sum and difference frequencies ($\upsilon = \upsilon_{FIR} \pm \upsilon_{MW}$). The tunable sideband radiation is separated from the much stronger residual THz center frequency radiation with a Michelson polarizing interferometer and is then directed to multipass optics that encompass the supersonic expansion. This supersonic expansion, formed by expanding 1−2 atm of a 0.5−1% mixture of NH_3 in Ar through a 4″ × 0.005″ slit nozzle, creates a beam of ammonia clusters with a temperature of about 4K. After passing ~8 times through the expansion, the radiation is detected by a liquid helium cooled stressed Ga:Ge photoconductor detector. The far-infrared laser lines used for this scan were 2409.2932 (±56) GHz (*trans*-CH_2F_2), 2447.9685 (±40) GHz (CD_3OH), 2522.7815 (±40) GHz (CH_3OH), 2546.4950 (±40) GHz (*trans*-CH_2F_2), 2633.8991 (±40) GHz ($^{13}CH_3OH$), and 2714.7151 (±40) GHz ($^{13}CH_3OH$).

Observed Spectra and Analysis. A total of more than 900 transitions were recorded with ca. 2 MHz precision. 282 were assigned to the six new $A + E$ vibration−rotation−tunneling

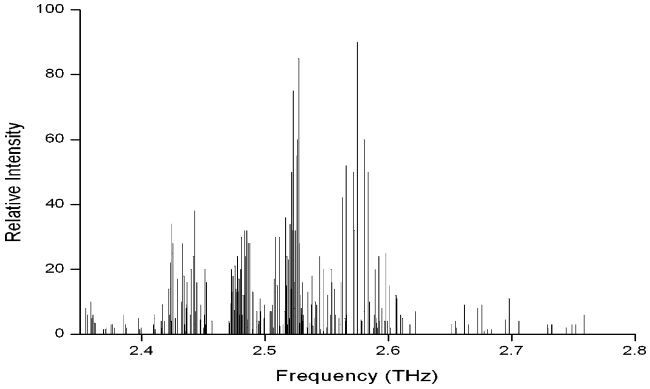

Figure 2. Stick spectrum of the assigned $A-E$ states transitions of $(NH_3)_2$.

states: a $K = 0$ stack of G_2^- symmetry 2585.6 GHz above the lowest $K = 0A + E$ state and a $K = 0$ stack of G_2^+ symmetry 2586.7 GHz above the lowest $K = 0A + E$ state, four $K = 1$ stacks of G_2^-/G_2^+ symmetry 2476.7, 2528.3, 2644.1, and 2812.5 GHz above the lowest $K = 0A + E$ state. Figure 2 is a stick spectrum of the assigned transitions for the *A-E* (*ortho-para*) state. The strongest transitions are in the pair of K=0 ← 1 (lower) subbands and the two pairs of K=1 ← 0 subbands terminating in the 2476.7 and 2528.3 GHz excited states. The pair of K=0 ← 1 (upper) subbands was also observed, but they were weaker because of their smaller Boltzmann weights at the 4K beam temperature. These six new excited states correspond to an out-of-plane mode and an in-plane mode. These transitions have been least-squares fit to the following energy level expressions using SPFIT:[23]

$$E = E_n + B_n J(J+1) - D_n(J(J+1))^2 \quad (1)$$

$$E(n,J,K,\pm) = E_n + B_n(J(J+1) - K^2) - D_n(J(J+1) - K^2)^2 \pm q_B \delta_{K,1} J(J+1) \quad (2)$$

Here, B is the rotational constant, D is the centrifugal distortion constant, q_B represents the parity doubling constant corresponding to asymmetry doubling, which is constrained to be positive in the fit. For the $K = 0$ ($K = 1$) manifold, expression 1 (2) is used. A Coriolis coupling constant c ($\approx 2\sqrt{2}B\zeta$) was used to account for the off-diagonal matrix elements between the two VRT levels of the same J and the same symmetry on $K = 0$ and 1. A combinational fit that treats the new THz transitions together with the previously reported ground state transitions, similar to what has been done to the $A-A$ (ortho−ortho) state THz transitions,[5] was attempted but not successful. The strong Coriolis couplings among not only the observed excited states but also between these states and the as yet unobserved $K = 2$ state precluded such a satisfactory global fit.

The Out-of-Plane Mode. 210 transitions were assigned to the two $K = 0$ stacks at 2585.6 and 2586.7 GHz above the lowest $K = 0$ $A + E$ state, and to two $K = 1$ stacks of G_2^-/G_2^+ symmetry at 2476.7 and 2528.3 GHz of an out-of-plane vibration, based on combination differences. These transitions are listed in Table 1 with their corresponding symmetries. Because of Coriolis coupling between the new $K =$ states and the 2528.3 GHz manifold, much weaker pairs of $K = 0 \leftarrow 0$ subbands and $K = 0 \leftarrow 0$ Q branches, as well as a $K = 1 \leftarrow 1$ (lower) subband were also observed. Also because of Coriolis coupling between the 2476.7 GHz $K = 1$ manifold and another unobserved manifold, a weaker $K = 1 \leftarrow 1$ subband was observed to this state as well. In the analysis of the ground state

TABLE 1: Measured Frequencies for the *A*−*E* (ortho−para) States of Ammonia Dimer for an Out-of-Plane Vibration

J'	sym.′	K'	n'	J''	sym.	K''	n''	frequency (MHz)	J'	sym.′	K'	n'	J''	sym.	K''	n''	frequency (MHz)
10	G_2^-	0	11	9	G_2^+	1	3	2590180	4	G_2^+	0	12	4	G_2^-	1	3	2476718
9	G_2^+	0	11	8	G_2^-	1	3	2577834	3	G_2^-	0	12	3	G_2^+	1	3	2475234
8	G_2^-	0	11	7	G_2^+	1	3	2565465	2	G_2^+	0	12	2	G_2^-	1	3	2474051
7	G_2^+	0	11	6	G_2^-	1	3	2553115	1	G_2^-	0	12	1	G_2^+	1	3	2473225
6	G_2^-	0	11	5	G_2^+	1	3	2540826	7	G_2^-	0	12	6	G_2^+	1	6	2436250
5	G_2^+	0	11	4	G_2^-	1	3	2528647	6	G_2^+	0	12	5	G_2^-	1	6	2423924
4	G_2^-	0	11	3	G_2^+	1	3	2516641	4	G_2^+	0	12	3	G_2^-	1	6	2399703
3	G_2^+	0	11	2	G_2^-	1	3	2504872	3	G_2^-	0	12	2	G_2^+	1	6	2387935
2	G_2^-	0	11	1	G_2^+	1	3	2493406	2	G_2^+	0	12	1	G_2^-	1	6	2376474
5	G_2^+	0	11	6	G_2^-	1	3	2415980	9	G_2^-	0	12	9	G_2^+	1	5	2369093
4	G_2^-	0	11	5	G_2^+	1	3	2424437	6	G_2^+	0	12	6	G_2^-	1	5	2362552
3	G_2^+	0	11	4	G_2^-	1	3	2433145	5	G_2^-	0	12	5	G_2^+	1	5	2360569
2	G_2^-	0	11	3	G_2^+	1	3	2442165	4	G_2^+	0	12	4	G_2^-	1	5	2358774
1	G_2^+	0	11	2	G_2^-	1	3	2451561	2	G_2^+	0	12	2	G_2^-	1	5	2356005
9	G_2^+	0	11	9	G_2^-	1	4	2485671	8	G_2^+	0	12	7	G_2^-	0	2	2677725
8	G_2^-	0	11	8	G_2^+	1	4	2483523	9	G_2^-	0	12	8	G_2^+	0	2	2512100
7	G_2^+	0	11	7	G_2^-	1	4	2481393	7	G_2^-	0	12	6	G_2^+	0	2	2528209
6	G_2^-	0	11	6	G_2^+	1	4	2479336	6	G_2^+	0	12	5	G_2^-	0	2	2536550
5	G_2^+	0	11	5	G_2^-	1	4	2477397	5	G_2^-	0	12	4	G_2^+	0	2	2545161
4	G_2^-	0	11	4	G_2^+	1	4	2475636	4	G_2^+	0	12	3	G_2^-	0	2	2554108
3	G_2^+	0	11	3	G_2^-	1	4	2474116	9	G_2^-	0	12	9	G_2^+	0	1	2601739
2	G_2^-	0	11	2	G_2^+	1	4	2472902	8	G_2^+	0	12	8	G_2^-	0	1	2599385
1	G_2^+	0	11	1	G_2^-	1	4	2472053	7	G_2^-	0	12	7	G_2^+	0	1	2597081
7	G_2^+	0	11	6	G_2^-	1	5	2435332	6	G_2^+	0	12	6	G_2^-	0	1	2594873
6	G_2^-	0	11	5	G_2^+	1	5	2422956	5	G_2^-	0	12	5	G_2^+	0	1	2592807
5	G_2^+	0	11	4	G_2^-	1	5	2410705	4	G_2^+	0	12	4	G_2^-	0	1	2590943
4	G_2^-	0	11	3	G_2^+	1	5	2398639	3	G_2^-	0	12	3	G_2^+	0	1	2589346
3	G_2^+	0	11	2	G_2^-	1	5	2386826	2	G_2^+	0	12	2	G_2^-	0	1	2588078
2	G_2^-	0	11	1	G_2^+	1	5	2375331	8	G_2^-	1	7	7	G_2^+	0	1	2578675
10	G_2^-	0	11	10	G_2^+	1	6	2370615	7	G_2^+	1	7	6	G_2^-	0	1	2564807
6	G_2^-	0	11	6	G_2^+	1	6	2361606	6	G_2^-	1	7	5	G_2^+	0	1	2551083
5	G_2^+	0	11	5	G_2^-	1	6	2359566	5	G_2^+	1	7	4	G_2^-	0	1	2537589
3	G_2^+	0	11	3	G_2^-	1	6	2356130	4	G_2^-	1	7	3	G_2^+	0	1	2524404
2	G_2^-	0	11	2	G_2^+	1	6	2354865	3	G_2^+	1	7	2	G_2^-	0	1	2511629
8	G_2^-	0	11	7	G_2^+	0	1	2680192	2	G_2^-	1	7	1	G_2^+	0	1	2499357
6	G_2^-	0	11	5	G_2^+	0	1	2655194	1	G_2^+	1	7	0	G_2^-	0	1	2487698
8	G_2^-	0	11	9	G_2^+	0	1	2506700	6	G_2^-	1	7	7	G_2^+	0	1	2418327
7	G_2^+	0	11	8	G_2^-	0	1	2514518	5	G_2^+	1	7	6	G_2^-	0	1	2425229
5	G_2^+	0	11	6	G_2^-	0	1	2530513	4	G_2^-	1	7	5	G_2^+	0	1	2432458
4	G_2^-	0	11	5	G_2^+	0	1	2538805	3	G_2^+	1	7	4	G_2^-	0	1	2440101
3	G_2^+	0	11	4	G_2^-	0	1	2547370	2	G_2^-	1	7	3	G_2^+	0	1	2448261
2	G_2^-	0	11	3	G_2^+	0	1	2556276	1	G_2^+	1	7	2	G_2^-	0	1	2457038
1	G_2^+	0	11	2	G_2^-	0	1	2565583	8	G_2^-	1	7	8	G_2^+	0	2	2493693
7	G_2^+	0	11	7	G_2^-	0	2	2592858	7	G_2^+	1	7	7	G_2^-	0	2	2490012
6	G_2^-	0	11	6	G_2^+	0	2	2590596	6	G_2^-	1	7	6	G_2^+	0	2	2486486
5	G_2^+	0	11	5	G_2^-	0	2	2588482	5	G_2^+	1	7	5	G_2^-	0	2	2483195
3	G_2^+	0	11	3	G_2^-	0	2	2584929	4	G_2^-	1	7	4	G_2^+	0	2	2480223
2	G_2^-	0	11	2	G_2^+	0	2	2583623	3	G_2^+	1	7	3	G_2^-	0	2	2477660
9	G_2^-	0	12	8	G_2^+	1	4	2578560	2	G_2^-	1	7	2	G_2^+	0	2	2475608
8	G_2^+	0	12	7	G_2^-	1	4	2566263	1	G_2^+	1	7	1	G_2^-	0	2	2474167
7	G_2^-	0	12	6	G_2^+	1	4	2553980	7	G_2^+	1	7	6	G_2^-	1	3	2450271
6	G_2^+	0	12	5	G_2^-	1	4	2541756	6	G_2^-	1	7	5	G_2^+	1	3	2436715
5	G_2^-	0	12	4	G_2^+	1	4	2529639	5	G_2^+	1	7	4	G_2^-	1	3	2423361
4	G_2^+	0	12	3	G_2^-	1	4	2517691	4	G_2^-	1	7	3	G_2^+	1	3	2410293
3	G_2^-	0	12	2	G_2^+	1	4	2505973	3	G_2^+	1	7	2	G_2^-	1	3	2397602
2	G_2^+	0	12	1	G_2^-	1	4	2494547	2	G_2^-	1	7	1	G_2^+	1	3	2385391
5	G_2^-	0	12	6	G_2^+	1	4	2416949	7	G_2^-	1	8	6	G_2^+	0	2	2561482
4	G_2^+	0	12	5	G_2^-	1	4	2425470	6	G_2^+	1	8	5	G_2^-	0	2	2547760
3	G_2^-	0	12	4	G_2^+	1	4	2434231	5	G_2^-	1	8	4	G_2^+	0	2	2534266
2	G_2^+	0	12	3	G_2^-	1	4	2443295	4	G_2^+	1	8	3	G_2^-	0	2	2521088
1	G_2^-	0	12	2	G_2^+	1	4	2452724	3	G_2^-	1	8	2	G_2^+	0	2	2508314
9	G_2^-	0	12	9	G_2^+	1	3	2486560	2	G_2^+	1	8	1	G_2^-	0	2	2496046
8	G_2^+	0	12	8	G_2^-	1	3	2484443	1	G_2^-	1	8	0	G_2^+	0	2	2484387
7	G_2^-	0	12	7	G_2^+	1	3	2482355	5	G_2^-	1	8	6	G_2^+	0	2	2421905
6	G_2^+	0	12	6	G_2^-	1	3	2480337	4	G_2^+	1	8	5	G_2^-	0	2	2429137
5	G_2^-	0	12	5	G_2^+	1	3	2478438	3	G_2^-	1	8	4	G_2^+	0	2	2436784

TABLE 1 (Continued)

J'	sym.′	K'	n'	J''	sym.	K''	n''	frequency (MHz)	J'	sym.′	K'	n'	J''	sym.	K''	n''	frequency (MHz)
2	G_2^+	1	8	3	G_2^-	0	2	2444948	2	G_2^-	1	9	2	G_2^+	0	2	2523932
1	G_2^-	1	8	2	G_2^+	0	2	2453726	1	G_2^+	1	9	1	G_2^-	0	2	2524603
7	G_2^-	1	8	7	G_2^+	0	1	2493324	9	G_2^+	1	9	8	G_2^-	1	3	2494965
6	G_2^+	1	8	6	G_2^-	0	1	2489794	8	G_2^-	1	9	7	G_2^+	1	3	2486333
5	G_2^-	1	8	5	G_2^+	0	1	2486502	7	G_2^+	1	9	6	G_2^-	1	3	2477791
4	G_2^+	1	8	4	G_2^-	0	1	2483530	4	G_2^-	1	9	3	G_2^+	1	3	2451874
3	G_2^-	1	8	3	G_2^+	0	1	2480968	3	G_2^+	1	9	2	G_2^-	1	3	2442923
2	G_2^+	1	8	2	G_2^-	0	1	2478916	3	G_2^+	1	9	4	G_2^-	1	3	2371194
1	G_2^-	1	8	1	G_2^+	0	1	2477475	9	G_2^-	1	10	8	G_2^+	0	2	2606918
7	G_2^-	1	8	6	G_2^+	1	4	2450222	8	G_2^+	1	10	7	G_2^-	0	2	2598037
6	G_2^+	1	8	5	G_2^-	1	4	2436678	7	G_2^-	1	10	6	G_2^+	0	2	2589264
5	G_2^-	1	8	4	G_2^+	1	4	2423334	6	G_2^+	1	10	5	G_2^-	0	2	2580507
4	G_2^+	1	8	3	G_2^-	1	4	2410276	5	G_2^-	1	10	4	G_2^+	0	2	2571704
3	G_2^-	1	8	2	G_2^+	1	4	2397593	4	G_2^+	1	10	3	G_2^-	0	2	2562791
2	G_2^+	1	8	1	G_2^-	1	4	2385387	3	G_2^-	1	10	2	G_2^+	0	2	2553713
9	G_2^+	1	9	8	G_2^-	0	1	2609911	2	G_2^+	1	10	1	G_2^-	0	2	2544412
8	G_2^-	1	9	7	G_2^+	0	1	2601060	1	G_2^-	1	10	0	G_2^+	0	2	2534839
7	G_2^+	1	9	6	G_2^-	0	1	2592326	8	G_2^+	1	10	9	G_2^-	0	2	2424536
6	G_2^-	1	9	5	G_2^+	0	1	2583613	7	G_2^-	1	10	8	G_2^+	0	2	2436124
5	G_2^+	1	9	4	G_2^-	0	1	2574854	6	G_2^+	1	10	7	G_2^-	0	2	2447747
4	G_2^-	1	9	3	G_2^+	0	1	2565985	4	G_2^+	1	10	5	G_2^-	0	2	2470838
3	G_2^+	1	9	2	G_2^-	0	1	2556945	3	G_2^-	1	10	4	G_2^+	0	2	2482183
2	G_2^-	1	9	1	G_2^+	0	1	2547682	2	G_2^+	1	10	3	G_2^-	0	2	2493313
1	G_2^+	1	9	0	G_2^-	0	1	2538137	1	G_2^-	1	10	2	G_2^+	0	2	2504178
9	G_2^+	1	9	10	G_2^-	0	1	2416076	9	G_2^-	1	10	9	G_2^+	0	1	2518405
8	G_2^-	1	9	9	G_2^+	0	1	2427566	8	G_2^+	1	10	8	G_2^-	0	1	2519696
7	G_2^+	1	9	8	G_2^-	0	1	2439191	7	G_2^-	1	10	7	G_2^+	0	1	2521104
6	G_2^-	1	9	7	G_2^+	0	1	2450857	6	G_2^+	1	10	6	G_2^-	0	1	2522542
4	G_2^-	1	9	5	G_2^+	0	1	2474036	5	G_2^-	1	10	5	G_2^+	0	1	2523936
3	G_2^+	1	9	4	G_2^-	0	1	2485421	4	G_2^+	1	10	4	G_2^-	0	1	2525232
2	G_2^-	1	9	3	G_2^+	0	1	2496585	3	G_2^-	1	10	3	G_2^+	0	1	2526366
1	G_2^+	1	9	2	G_2^-	0	1	2507475	2	G_2^+	1	10	2	G_2^-	0	1	2527281
9	G_2^+	1	9	9	G_2^-	0	2	2514749	1	G_2^-	1	10	1	G_2^+	0	1	2527928
8	G_2^-	1	9	8	G_2^+	0	2	2516080	9	G_2^-	1	10	8	G_2^+	1	4	2495224
7	G_2^+	1	9	7	G_2^-	0	2	2517533	8	G_2^+	1	10	7	G_2^-	1	4	2486575
6	G_2^-	1	9	6	G_2^+	0	2	2519016	7	G_2^-	1	10	6	G_2^+	1	4	2478004
5	G_2^+	1	9	5	G_2^-	0	2	2520460	3	G_2^-	1	10	2	G_2^+	1	4	2442992
4	G_2^-	1	9	4	G_2^+	0	2	2521802	5	G_2^-	1	10	5	G_2^+	1	3	2409570
3	G_2^+	1	9	3	G_2^-	0	2	2522979	9	G_2^-	1	10	8	G_2^+	1	5	2377736

VRT spectra of the $A + E$ states, Loeser et al.[4] observed transitions involving the $K = 2$ state and included them in their analysis to achieve a good fit, so it is likely that the missing manifold here is likewise a $K = 2$ manifold. Several approaches were attempted to treat these transitions. In Trial 1, we analyzed the data neglecting Coriolis perturbations, and instead added higher centrifugal distortion terms, using the expression

$$E = E_n + B_n J(J+1) - D_n(J(J+1))^2 + H_n(J(J+1))^3 + L_n(J(J+1))^4 \cdots \quad (3)$$

The two degenerate K=1 states were allowed to fit B, D, H, and L independently, only fixed at the same energy. The spectroscopic constants resulting from this are given in Table 2. These high-order distortion constants do not reflect any physical property of $(NH_3)_2$, but are merely fitting parameters.[24] If a $K = 0$ and a nearby $K = 1$ manifold are Coriolis coupled with no other interactions, it should be possible to use only B and D in the energy level expression and off-diagonal Coriolis matrix elements between the levels of the same J and the same symmetry. Unfortunately, as will be discussed below, this deperturbation was not successful. In trial 2, we added the Coriolis coupling constant between the 2528.3 GHz $K = 1$ state and the $K = 0$ states, but only included a portion of the transitions that were not heavily affected by the other perturbations. It is evident from the large centrifugal distortion constants obtained for all the observed excited states that Coriolis interactions are indeed very important in these $A-E$ states in Trial 1 and 2. The experimental precision was set at 2 MHz in these fits, and all the transitions were weighted equally. The fitted constants from Trial 2 are listed in Table 3. The quality of the fit suffered from the very strong Coriolis coupling effects. The Coriolis coupling constant between the $K = 1$ state and $K = 0$ state is 4562 MHz in Trial 2, which indicates a very strong Coriolis interaction between the $K = 0$ and 2528.3 GHz $K = 1$ states. This Coriolis coupling constant is a factor of 2∼3 times larger than the corresponding ground state Coriolis coupling constants, so that Coriolis interactions over larger energy gaps have a significant effect on the rotational constants too. The consequence is that the deperturbed rotational constants, which might contain useful physical information about the upper state vibrations, cannot yet be considered in this analysis. The effects of the Coriolis couplings also caused the energy levels of the two new $K = 1$ states to be situated lower than the $K = 0$ states. It is very possible that the 2476.7 GHz $K = 1$ state is also involved in the coupling with the $K = 0$ states, aside from the

TABLE 2: Spectroscopic Constants for the *A*−*E* (ortho−para) States of Ammonia Dimer for an Out-of-Plane Vibration without Treatment of Perturbations

state			state		
7, 8	$E_{7,8}$/MHz	2476732.41 (98)	9, 10	$E_{9,10}$/MHz	2528260.49 (91)
7	*B*/MHz	5486.66 (31)	9	*B*/MHz	4935.08 (19)
	D/kHz	2154 (25)		*D*/kHz	−945.0 (97)
	H/kHz	16.39 (71)		*H*/kHz	−5.21 (17)
	L/kHz	−0.0772 (64)		*L*/kHz	0.0200 (96)
8	*B*/MHz	5486.28	10	*B*/MHz	4941.91 (19)
	D/kHz	2146 (25)		*D*/kHz	−890.4 (97)
	H/kHz	16.22 (71)		*H*/kHz	−4.94 (17)
	L/kHz	−0.0754 (64)		*L*/kHz	0.0193 (96)
11	E_{11}/MHz	2585556.0 (16)	12	E_{12}/MHz	2586739.9 (12)
	B/MHz	5346.09 (30)		*B*/MHz	5338.94 (23)
	D/kHz	1118 (14)		*D*/kHz	1058 (11)
	H/kHz	5.12 (25)		*H*/kHz	4.58 (18)
	L/kHz	−0.0143 (13)		*L*/kHz	0.127 (10)

TABLE 3: Spectroscopic Constants for the *A*−*E* (ortho−para) States of Ammonia Dimer for an Out-of-Plane Vibration (from Deperturbation Analysis)

state				Loeser et al.[a]
1	*B*/MHz	5110.58 (22)	5110.575 (66)	5110.41054 (47)
	D/kHz	54.0 (20)	53.44 (61)	52.683 (49)
2	E_2/MHz	3308.5 (29)	3309.57(87)	3309.41 (26)
	B/MHz	5110.66 (22)	5110.726 (66)	5110.56116 (48)
	D/kHz	51.9 (22)	53.22 (66)	52.478 (51)
3, 4	$E_{3,4}$/MHz			113938.33 (38)
	B/MHz			5125.420 (12)
	D/kHz			60.599 (80)
	qB/MHz			0.4920 (20)
5, 6	$E_{5,6}$/MHz			232026.98 (54)
	B/MHz			5117.218 (19)
	D/kHz			53.93 (14)
	qB/MHz			0.1536 (33)
7, 8	$E_{7,8}$/MHz		2476732.41	
	B/MHz		5486.44	
	D/kHz		1.98	
	qB/MHz		3.43	
9, 10	$E_{9,10}$/MHz	2528266.4 (25)	2528258.57 (74)	
	B/MHz	5117.1 (60)	5211.4 (80)	
	D/kHz	284.9 (40)	-184.9 (37)	
	qB/MHz	2.268 (32)	2.077 (26)	
11	E_{11}/MHz	2585560.3 (40)	2585555.24 (126)	
	B/MHz	5164.2 (60)	5067.18 (123)	
	D/kHz	420.5 (51)	525.7 (53)	
12	E_{12}/MHz	2586747.2 (49)	2586738.39 (165)	
	B/MHz	5160.6 (60)	5065.55 (115)	
	D/kHz	407.9 (60)	521.3 (73)	
	$c_{9,11}$= $c_{10,12}$/MHz	4562 (79)	5475.8 (137)	
	$c_{7,11}$= $c_{8,12}$/MHz		1980	
	N	74	74	
	σ/MHz	5.3	2.0	

[a] Reference 4.

fact that this state is even more perturbed by another nearby state, which lies at lower energy. In Trial 3, we added the Coriolis coupling constant between the 2476.7 GHz $K = 1$ state and the $K = 0$ states, with the other constants for that state fixed at the values from Trial 1. Even though the resulting rms of this fit fell within the experimental error, the centrifugal distortion constants for these three states were still larger than are reasonable and the sign of the centrifugal distortion constant for 2528.3 GHz $K = 1$ states was also incorrect. Attempts to characterize this elusive perturbing state from its effects on the observed 2476.7 GHz $K = 1$ state or its effects on both 2476.7 GHz $K = 1$ state and the $K = 0$ states, were not successful. The fitted constants from Trial 3 are also listed in Table 3. Figure 3 displays the energy level diagram for the assigned VRT states of the *A*−*E* (ortho−para) state for this out-of-plane vibration.

The In-Plane Mode. 72 transitions were assigned to the two $K = 1$ stacks of G_2^-/G_2^+ symmetry at 2644.1 and 2812.5 GHz, based on combination differences. These transitions are listed in Table 4 with their symmetries. The rotational levels can be fit up to $J = 6$ with only the *B* rotational constant and small *D* centrifugal distortion constants. These $K = 1$ excited states do not appear to be Coriolis-coupled to the 2586 GHz $K = 0$ states, even though they lie as close to them as do the 2812.5 GHz $K = 1$ states. These two states are assigned to the in-plane vibration. The assignment of this vibration is discussed in the next section. For the rotational levels with $J > 6$, there is a shift that cannot be mathematically described by polynomials in $J(J+1)$. Including higher order distortion terms gave no improvement. These transitions were thus excluded from the fit. The fitted constants for these new states are listed in Table 5. We note that these $K = 1$ excited states

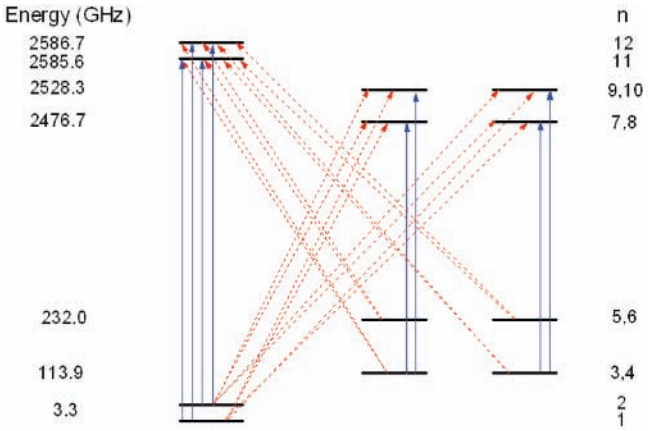

Figure 3. The VRT energy levels for the out-of-plane vibration observed in this study. The dashed arrows indicate perpendicular bands, solid arrows correspond to parallel bands.

do not appear to be Coriolis-coupled to the $K = 0$ excited states, even though the 2644.1 GHz $K = 1$ state is as close to them as is the 2528.3 GHz $K = 1$ state. More transitions from other states of this vibration are needed to converge the fit and to fully characterize the nature of this vibration. Figure 4 is the energy level diagram of the assigned VRT states of the $A-E$ (ortho−para) state for this in-plane vibration.

TABLE 5: Spectroscopic Constants for the $A-E$ (ortho−para) States for an In-Plane Vibration

13, 14	$E_{13,14}$/MHz	2644128.3 (113)
13	B/MHz	5199.62 (78)
	D/kHz	31.3 (91)
14	B/MHz	5200.14 (78)
	D/kHz	29.8 (91)
15, 16	$E_{15,16}$/MHz	2812533.4 (15)
15	B/MHz	5140.34 (16)
	D/kHz	34.5 (29)
16	B/MHz	5140.75 (16)
	D/kHz	34.0 (29)

Discussion

The inversion-tunneling splitting of the ammonia monomer that correlates to the E symmetry of the monomer rovibronic state was directly measured in this new THz study. The 1184 MHz spacing between the two new $K = 0$ states corresponds to the inversion splitting for the E monomer. This is a factor of 3 decrease from the lowest ground state splitting (3309 MHz) and a factor of 2 decrease from the upper interchange ground state splitting (2392 MHz). This shows that the new excited $A-E$ state wave functions are more localized than are the ground state $A-E$ wave functions. Olthof et al.[12] calculated the splittings due to umbrella inversion of the *para* monomer in the ammonia

TABLE 4: Measured Frequencies for the $A-E$ (ortho−para) States of Ammonia Dimer for an In-Plane Vibration

J'	sym.′	K'	n'	J''	sym.	K''	n''	frequency (MHz)	J'	sym.′	K'	n'	J''	sym.	K''	n''	frequency (MHz)
9	G_2^+	1	13	8	G_2^-	0	1	2744149[a]	3	G_2^-	1	14	2	G_2^+	1	4	2561834
8	G_2^-	1	13	7	G_2^+	0	1	2732365[a]	2	G_2^+	1	14	1	G_2^-	1	4	2551139
5	G_2^+	1	13	4	G_2^-	0	1	2697903	1	G_2^-	1	14	2	G_2^+	1	4	2509838
3	G_2^+	1	13	2	G_2^-	0	1	2675860	2	G_2^+	1	14	3	G_2^-	1	4	2499885
2	G_2^-	1	13	1	G_2^+	0	1	2665106	3	G_2^-	1	14	4	G_2^+	1	4	2490092
1	G_2^+	1	13	0	G_2^-	0	1	2654527	4	G_2^+	1	14	5	G_2^-	1	4	2480459
8	G_2^-	1	13	7	G_2^+	1	3	2617640[a]	5	G_2^-	1	14	6	G_2^+	1	4	2470986
7	G_2^+	1	13	6	G_2^-	1	3	2606098	7	G_2^-	1	14	8	G_2^+	1	4	2452522[a]
6	G_2^-	1	13	5	G_2^+	1	3	2594825	8	G_2^+	1	14	9	G_2^-	1	4	2443646[a]
5	G_2^+	1	13	4	G_2^-	1	3	2583678	9	G_2^-	1	14	10	G_2^+	1	4	2434829[a]
4	G_2^-	1	13	3	G_2^+	1	3	2572680	1	G_2^-	1	14	1	G_2^+	1	3	2530341
3	G_2^+	1	13	2	G_2^-	1	3	2561834	2	G_2^+	1	14	2	G_2^-	1	3	2530641
2	G_2^-	1	13	1	G_2^+	1	3	2551139	3	G_2^-	1	14	3	G_2^+	1	3	2531097
1	G_2^+	1	13	2	G_2^-	1	3	2509843	7	G_2^+	1	15	8	G_2^-	0	1	2732610[a]
2	G_2^-	1	13	3	G_2^+	1	3	2499894	5	G_2^+	1	15	6	G_2^-	0	1	2752170
3	G_2^+	1	13	4	G_2^-	1	3	2490105	4	G_2^-	1	15	3	G_2^+	1	3	2621902
4	G_2^-	1	13	5	G_2^+	1	3	2480476	3	G_2^+	1	15	2	G_2^-	1	3	2611484
5	G_2^+	1	13	6	G_2^-	1	3	2471010	2	G_2^-	1	15	1	G_2^+	1	3	2601113
7	G_2^+	1	13	8	G_2^-	1	3	2452558[a]	1	G_2^+	1	15	1	G_2^-	1	4	2580552
8	G_2^-	1	13	9	G_2^+	1	3	2443691[a]	6	G_2^-	1	15	7	G_2^+	1	3	2509950
9	G_2^+	1	13	10	G_2^-	1	3	2434878[a]	4	G_2^-	1	15	5	G_2^+	1	3	2529826
1	G_2^+	1	13	1	G_2^-	1	4	2530337	3	G_2^+	1	15	4	G_2^-	1	3	2539860
2	G_2^-	1	13	2	G_2^+	1	4	2530632	2	G_2^-	1	15	3	G_2^+	1	3	2549945
3	G_2^+	1	13	3	G_2^-	1	4	2531078	1	G_2^+	1	15	2	G_2^-	1	3	2560082
8	G_2^+	1	14	7	G_2^-	0	2	2729091[a]	7	G_2^-	1	16	8	G_2^+	0	2	2729313
6	G_2^+	1	14	5	G_2^-	0	2	2705901	5	G_2^-	1	16	6	G_2^+	0	2	2748867
5	G_2^-	1	14	4	G_2^+	0	2	2694607	4	G_2^+	1	16	5	G_2^-	0	2	2758756
4	G_2^+	1	14	3	G_2^-	0	2	2683490	4	G_2^+	1	16	3	G_2^-	1	4	2621915
3	G_2^-	1	14	2	G_2^+	0	2	2672557	3	G_2^-	1	16	2	G_2^+	1	4	2611491
2	G_2^+	1	14	1	G_2^-	0	2	2661800	2	G_2^+	1	16	1	G_2^-	1	4	2601116
1	G_2^-	1	14	0	G_2^+	0	2	2651222	1	G_2^-	1	16	1	G_2^+	1	3	2580552
8	G_2^+	1	14	7	G_2^-	1	4	2617629[a]	6	G_2^+	1	16	7	G_2^-	1	4	2509968
7	G_2^-	1	14	6	G_2^+	1	4	2606091	4	G_2^+	1	16	5	G_2^-	1	4	2529847
6	G_2^+	1	14	5	G_2^-	1	4	2594821	3	G_2^-	1	16	4	G_2^+	1	4	2539871
5	G_2^-	1	14	4	G_2^+	1	4	2583676	2	G_2^+	1	16	3	G_2^-	1	4	2549951
4	G_2^+	1	14	3	G_2^-	1	4	2572680	1	G_2^-	1	16	2	G_2^+	1	4	2560085

[a] Excluded from the fit. See text for detail.

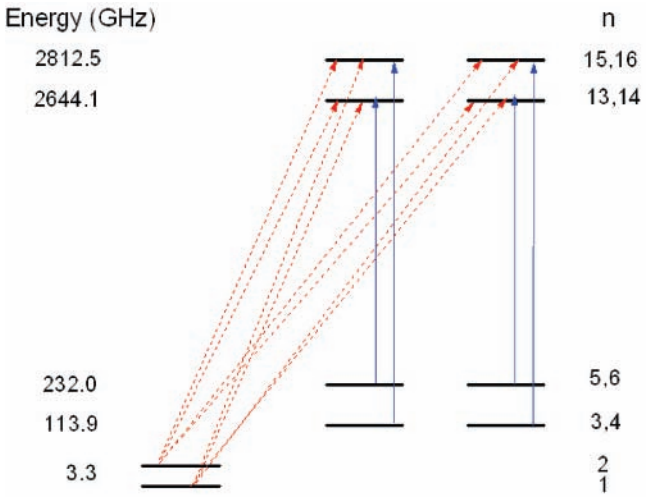

Figure 4. The VRT energy levels for the in-plane vibration observed in this study. The dashed arrows indicate perpendicular bands, solid arrows correspond to parallel bands.

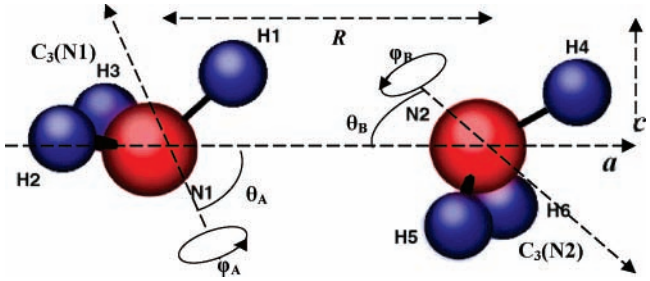

Figure 5. The internal coordinate system of the ammonia dimer. R is the distance between the centers of mass of the two monomers. θ_A and θ_B are the angles between the monomer C_3 axes and the a-axis. φ_A and φ_B describe the internal rotation of the monomers about their C_3 axes, and γ is the dihedral angle between the two C_3 axes, The a and c inertial axes lie in the assumed plane of symmetry.

dimer and discussed the nature of the inversion-tunneling. They found that the largest inversion splittings occur for the $A-E$ states with $K = 0$, because they originate from the inversion tunneling of the para monomer through a true first-order mechanism, whereas for the $K = 1$ state, they are introduced by an indirect mechanism through Coriolis coupling.

The ammonia dimer can be described by six intermolecular coordinates, as illustrated in Figure 5, with the a and c inertial axes lying in the assumed plane of symmetry. The three in-plane coordinates are R, the distance between the centers of mass of the two monomers, and θ_A and θ_B, the angles between the monomer C_3 axes and the a-axis, respectively. The three out-of-plane coordinates are φ_A and φ_B, which describe the internal rotation of the monomers about their C_3 axes, and γ, the dihedral angle between the two C_3 axes. Assuming the restoring forces in θ_A and θ_B to be similar, as well as those for φ_A and φ_B, there should be three in-plane intermolecular vibrations. They are the intermolecular stretch in the R coordinate; the 'trans' in-plane bend in the $\theta_A - \theta_B$ coordinate; and the "cis" in-plane bend in the $\theta_A + \theta_B$ coordinate. There should also be three out-of-plane intermolecular vibrations. They are the out-of-plane torsion in the γ coordinate; the "geared" out-of-plane twist in the $\varphi_A + \varphi_B$ coordinate; and the "anti-geared" out-of-plane twist in the $\varphi_A - \varphi_B$ coordinate. To our knowledge, only the harmonic frequencies for the intermolecular modes of the ammonia dimer have been calculated from various potential energy surfaces, including the results from Marsden,[25] Dykstra and Andrews,[26] Frisch et al.[27], Muguet et al.[28], Bende et al.[29], and Altmann et al.[30]. The ab initio harmonic vibrational frequencies are known to be often too high for the weakly bound systems. The six dimensional dynamics calculation carried out by the van der Avoird group[16] did not include the higher energy eigenstates. That kind of calculation, even if the model potential was not perfect, would be far more reliable for such a floppy system. In our previous analysis of the $A-A$ state transitions, we assign the transitions to half of the interchange tunneling sublevels of an out-of-plane vibration. We assume that the $A-E$ state transitions discussed here correspond to the same out-of-plane vibration. We note that the ordering of G_2^- and G_2^+ levels are not reversed with respect to the ground state ordering. The A_3 irreducible representation of $\mathbf{G_{36}}$ correlates to $A_1^- \oplus E^+ \oplus B_2^-$ in $\mathbf{G_{144}}$. Multiplying the ground state ordering of the $A+E$ states (G_1^+, G_1^-, G_2^-, G_2^+) by an intermolecular vibration of A_1^- symmetry in $\mathbf{G_{144}}$ gives an excited-state ordering (G_1^-, G_1^+, G_2^+, G_2^-) in which the G_2^- and G_2^+ levels are reversed with respect to the ground state ordering. Multiplying the ground state ordering by an intermolecular vibration of B^- symmetry in $\mathbf{G_{144}}$ gives an excited-state ordering (G_2^-, G_2^+, G_1^+, G_1^-) in which the G_2^- and G_2^+ levels are not reversed with respect to the ground state ordering, which explains the present observations.

Extensive continuous spectral coverage at higher frequency is needed in order to study how the interchange motion is affected by this intermolecular out-of-plane vibration. This extension will also yield more information on the in-plane vibration discussed here. Of the possible in-plane modes, the antigeared in-plane bend is predicted to lie 4 times higher in energy by the harmonic calculations, whereas for the van der Waals stretch vibration, we expect a noticeable decrease in B rotational constants with respect to the ground state, which is not observed here. Hence, by elimination, only the geared in-plane bend remains as a good candidate for this assignment. Since this motion is in the interchange coordinates, we expect the interchange frequency to increase substantially. We have also measured many transitions for the E-E VRT states of this out-of-plane vibration.[24] At present, the assignment is incomplete, suffering from exceptionally strong Coriolis interactions and yet more complicated tunneling dynamics, which require more extensive spectral coverage to obtain the requisite new data to complete this analysis. Nevertheless, we hope that the present study will motivate detailed study of the ammonia dimer by a similar combination of state of the art dynamics and potential models, such as the ones recently published for the water dimer.[10,12] This would greatly accelerate our understanding of this important prototype system.

Acknowledgment. This work was supported by Experimental Physical Chemistry Division of the National Science Foundation.

References and Notes

(1) Nelson, D. D. Jr.; Fraser, G. T.; Klemperer, W. *J. Chem. Phys.* **1985**, *83*, 6201.
(2) Nelson, D. D., Jr.; Klemperer, W. *J. Chem. Phys.* **1987**, *87*, 139.
(3) Nelson, D. D., Jr.; Klemperer, W.; Fraser, G. T.; Lovas, F. J. Suenram, R. D. *J. Chem. Phys.* **1987**, *87*, 6364.
(4) Loeser, J. G.; Schmuttenmaer, C. A.; Cohen, R. C.; Elrod, M. J.; Steyert, D. W.; Saykally, R. J.; Bumgarner, R. E.; Blake, G. A. *J. Chem. Phys.* **1992**, *97*, 4727.
(5) Lin, W.; Han, J-x.; Takahashi, L. K.; Loeser, J. G.; Saykally, R. J. *J. Phys. Chem. A* **2006**, *110*, 8011.
(6) Braly, L. B.; Cruzan, J. D.; Liu, K.; Fellers, R. S.; Saykally, R. J. *J. Chem. Phys.* **2000**, *112*, 10293.
(7) Braly, L. B.; Liu, K.; Brown, M. G.; Keutsch, F. N.; Fellers, R. S.; Saykally, R. J. *J. Chem. Phys.* **2000**, *112*, 10314.

(8) Keutsch, F. N.; Braly, L. B.; Brown, M. G.; Harker, H. A.; Petersen, P. B.; Leforestier, C.; Saykally, R. J. *J. Chem. Phys.* **2003**, *119*, 8927.

(9) Keutsch, F. N.; Goldman, N.; Harker, H. A.; Leforestier, C.; Saykally, R. J. *Mol. Phys.* **2003**, *101*, 3477.

(10) Leforestier, C.; Gatti, F.; Fellers, R. S.; Saykally, R. J. *J. Chem. Phys.* **2002**, *117*, 8710.

(11) Scribano, Y.; Goldman, N.; Saykally, R. J.; Leforestier, C. *J. Phys. Chem. A* **2006**, *110*, 5411.

(12) Bukowski, R.; Szalewicz, K.; Groenenboom, G. C.; van der Avoird, A. *Science*, **2007**, 315 1249.

(13) Boese, A. D.; Chandra, A.; Martin, J. M. L.; Marx, D. *J. Chem. Phys.* **2003**, *119*, 5965.

(14) Loeser, J. G. *Faraday Discuss. Chem. Soc*. **1994**, *97*, 159.

(15) Coudert, L. H.; Hougen J. T. *J. Mol. Spectrosc.* **1991**, *149*, 73.

(16) Olthof, E. H. T.; van der Avoird, A.; Wormer, P. E. S. *J. Chem. Phys.* **1994**, *101*, 8430.

(17) Olthof, E. H. T.; van der Avoird, A.; Wormer, P. E. S.; Loeser, J. G.; Saykally, R. J. *J. Chem. Phys.* **1994**, *101*, 8443.

(18) Müller-Dethlefs, K.; Hobza, P. *Chem. Rev.* **2000**, *100*, 143.

(19) Havenith, M. *Infrared Spectroscopy of Molecular Clusters*; Springer Verlag: Berlin, 2002; Chapter 9.

(20) Bunker, P. R.; Jensen, P. *Molecular Symmetry and Spectroscopy*, 2nd ed.; NRC Research Press: Ottawa, Canada, 1998; p 579.

(21) Saykally, R. J. *Acc. Chem. Rev.* **1989**, *22*, 295.

(22) Cohen, R. C.; Saykally, R. J. *J. Phys. Chem.* **1992**, *96*, 1024.

(23) Pickett, H. M. *J. Mol. Spectrosc.* **1991**, *148*, 371. The SPCAT and SPFIT spectroscopic predicting and fitting programs are available as free downloads from http://spec.jpl.nasa.gov/.

(24) Loeser, J. G. Ph.D. Dissertation, University of California at Berkeley, Berkeley, CA, 1995.

(25) Marsden, C. J. Private communication, 1991.

(26) Dykstra, C. E.; Andrews, L. *J. Chem. Phys.* **1990**, *92*, 6043.

(27) Frisch, M. J.; Bene, J. E. del; Binkley, J. S.; Schaefer, H. F., III. *J. Chem. Phys.* **1986**, *84*, 2279.

(28) Muguet, F. F.; Robinson, G. W.; Bassez-Muguet, M. P. *J Chem. Phys.* **1995**, *102*, 3655.

(29) Bende, A.; Vibók, Á.; Halász, G. J.; Suhai, S. *Int. J. Quantum Chem.* **2004**, *99*, 585.

(30) Altmann, J. A.; Govender, M. G.; Ford, T. A. *Mol. Phys*. **2005**, *103*, 949.